Available online at www.sciencedirect.com

ScienceDirect

Procedia Structural Integrity 2 (2016) 2068–2075

Structural Integrity Procedia

www.elsevier.com/locate/procedia

21st European Conference on Fracture, ECF21, 20-24 June 2016, Catania, Italy

CTOD estimation procedure for clad pipe girth welds subjected to bending load

Rodolfo F. de Souza[a,*], Claudio Ruggieri[b], Zhilhiang Zhang[c]

[a] *University of Sao Paulo, PVN-EPUSP, Sao Paulo, Brazil*
[b] *University of Sao Paulo, PVN-EPUSP, Sao Paulo, Brazil*
[c] *Norwegian University of Science and Technology, NTNU, Trondheim, Norway*

Abstract

This work describes a crack driving force estimation procedure applicable for structural integrity assessments of dissimilar girth welds in clad pipes subjected to high levels of bending load. The purpose of this study is to explore the application of the equivalent stress-strain relationship approach coupled with a weld bevel simplification scheme and the EPRI procedure to evaluate the CTOD for defects located at the weld centerline, including the effects of the weld strength mismatch, weld bevel geometry and the clad layer thickness. Parametric 3D finite element analyses of pipes with circumferential part-through cracks are performed to validate the weld joint simplification and to assess the accuracy of the crack driving forces predictions. Finally, the results show that the estimations using the proposed methodology are in close agreement to those obtained directly from finite element analyses.

Peer-review under responsibility of the Scientific Committee of ECF21.

Keywords: Weld Strength Mismatch; Pipeline Girth Welds; CTOD; ECA Procedures

1. Introduction

Structural integrity assessment of offshore pipelines conducting highly corrosive fluids has become a challenging engineering issue due to the increasing oil and gas production in harsh service conditions, such as very deep water offshore reservoirs. Ongoing technology developments support the use of C-Mn steel pipelines with a internal corrosion resistance alloy (CRA) layer, which is either metallurgically bonded to the outer pipe (clad pipe) or held in place by interference stress (lined pipe). While effective against corrosion, they require the use of CRA filler to produce field girth welds thereby introducing additional complexity in fracture assessments and specifications of critical crack sizes due to the dissimilar mechanical properties of the materials.

Moreover, offshore pipelines are subjected to severe installation conditions to enhance the operational productivity and reduce field development costs. A case of interest is the reel-lay method, in which the welded flowline is coiled around a large diameter reel on a vessel and transported to the deployment location into the sea where the pipe is

* Corresponding author.
E-mail address: rofigueira.souza@usp.br

Peer review under responsibility of the Scientific Committee of ECF21.
10.1016/j.prostr.2016.06.259

unreeled, straightened and finally layed to the sea floor. The main advantage of this method lies in onshore welding and inspection of the pipeline which allow very high quality welded joints in comparison to traditional laying techniques (Manouchehri, 2012). While fast and cost effective, the reel-lay installation subjects the pipe to large plastic deformations up to 4% which may complicate significantly accurate integrity assessments and fracture predictions.

Engineering critical assessment (ECA) procedures currently available, such as BS7910 (British Institution, 2013) and API579 (American Petroleum Institute, 2007) have been widely employed to assess the integrity of components under low levels of plasticity and made of homogeneous materials. However, they do not necessarily provide accurate assessments for large-scale yielding conditions and heteregoneus welded joints. Furthermore, the application of new high strength steels with corrosion resistant alloys favor the presence of weld strength undermatch or partial mismatch which thus raise strong concerns in integrity assessments of field girth welds having circumferential flaws.

This work adressess the development of a crack driving force estimation procedure for circumferential surface part-through external cracks in girth welds of clad pipes under bending load, based upon the equivalent stress-strain relationship approach proposed by Lei and Ainsworth (1997) coupled with a weld bevel simplification scheme (Hertelé et al., 2014) and the tradicional EPRI (Kumar et al., 1981) methodology. A case study is performed to evaluate the accuracy of the proposed method.

2. The equivalent stress and strain relationship method

The equivalent stress-strain relationship approach (ESSRM), proposed by Lei and Ainsworth (1997), treats the mechanical response of an idealized bimaterial welded joint in terms of an equivalent stress-plastic strain relationship that incorporates the influence of the weld joint geometry and material strength mismatch. The ESSRM is defined as

$$\sigma_{eq}(\varepsilon_p) = \left[\frac{P_0^{mism} - P_0^{bm}}{P_0^{wm} - P_0^{bm}}\right]\sigma_{wm}(\varepsilon_p) + \left[\frac{P_0^{wm} - P_0^{mism}}{P_0^{wm} - P_0^{bm}}\right]\sigma_{bm}(\varepsilon_p) \tag{1}$$

where P_0^{mism} denotes the limit load of the idealized bimaterial welded joint, P_0^{bm} and P_0^{wm} represent the limit load for the homogeneous component made of the base material and weld metal. The procedure described above requires only the specification of a proper limit load for the idealized bimaterial welded joint once all other quantities entering directly into the calculation of $\sigma(\varepsilon_p)$ are defined. Thus, using the new stress-strain curve which incorporates all the inhomogeneities of the weld (geometrical and mechanical), the crack driving force (CDF) estimation can simply be performed by adopting an adequate procedure applicable for homogeneous structures such as the EPRI methodology (Kumar et al., 1981).

2.1. EPRI estimation scheme for homogeneous pipes under bending

For a circumferentially cracked pipe subjected to bending (see Fig. 1), the CTOD can be expressed as the sum of the elastic and plastic components ($\delta = \delta_e + \delta_p$). The elastic component, δ_e, is determined by linear elastic fracture mechanics (Chiodo and Ruggieri, 2010) and the plastic component, δ_p, is expressed as

$$\delta_p = \alpha\epsilon_{ys} b\left[h_2(\frac{a}{t},\ \frac{D_e}{t},\ \theta,\ n)\right]\left(\frac{M}{M_0}\right)^{n+1} \tag{2}$$

where α is a dimensionless constant, n defines the strain hardening exponent of the material following a Ramberg-Osgood behavior (Anderson, 2005), σ_{ys} and $\epsilon_{ys} = \sigma_{ys}/E$ define the yield stress and strain, D_e is the pipe (cylinder) outer diameter, t is the wall thickness, $b = t - a$ defines the uncracked ligament, M_0 is the limit load of the cracked pipe configuration defined by API579 (2007), M denotes the applied bending moment and c is the circumferential crack half-length. In the above expression, h_2 is a dimensionless factor dependent upon crack size, component geometry and strain hardening properties of the material. Chiodo and Ruggieri (2010) describe in detail the h_2-factors evaluation procedure.

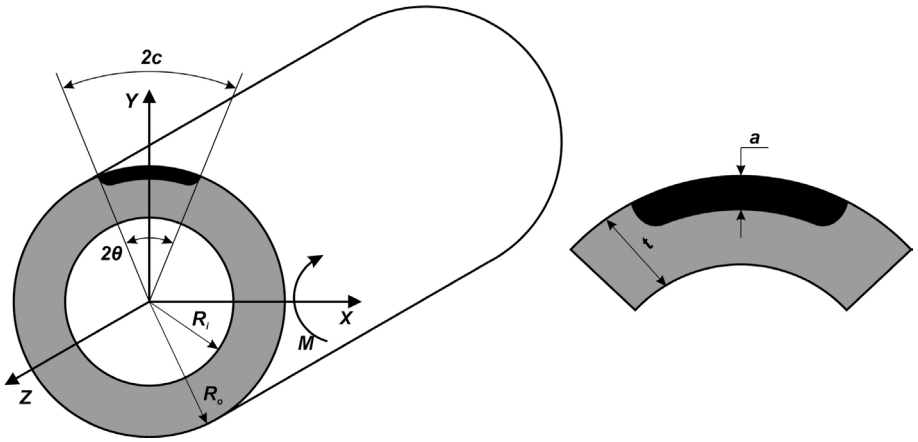

Fig. 1. Circumferentially cracked pipe under bending.

3. Limit load solution and weld geometry simplification procedure

The application of the ESSRM requires a proper definition of the limit load for the structural component, P_0^{mism}. Limit load solutions applicable to cracked pipes currently available in the literature cover a wide range of geometries, crack configurations and loading modes. However, there are no specific solutions for circumferential external surface part-through cracks in the girth weld of pipes or cylinders under bending load. Moreover, most of the available solutions in the literature consider an idealised rectangular weld bevel geometry (Kim et al., 2009) so that its application to an actual V-groove weld configuration can not be performed in a straightforward manner. To overcome this difficulties, the following strategy is adopted in this work:

- the V-groove weld geometry is simplified to a square weld;
- the limit load solution for pipes with finite circumferential part-through internal crack at the girth weld subjected to tension load (Kim et al., 2009) is adopted, as long as it describes accurately the limit load of the structure adopted in this work for mismatch levels within the range $M_y = \pm 20\%$ (Souza et al., 2016), where, $M_y = \sigma_{yw}/\sigma_{yb}$, in which σ_{yw} and σ_{yb} are the yield stress of the weld and base material respectively.

The weld geometry simplification follows from the work of Hertelé et al. (2014), where a procedure to compute the equivalent weld strip width for weld centerline cracks in single edge notched tension specimens (SENT or SE(T)) is proposed based on the slip-line patterns and their relationship with the loading bearing capacity of the structure. Considering the well established similarity between the evolution of crack tip stress triaxiality (and, therefore, the deformation pattern) of SENT specimens and pipes with external surface cracks at the girth weld loaded in bending load (Chiesa et al., 2001), it is assumed that the methodology developed by Hertelé et al. (2014) can be extended to the analysis of pipeline girth welds with circumferential surface part-through cracks.

Consider the pipe girth weld cross-section at the deepest point of the crack illustrated in Fig. 2(a). Assuming a straight slip-line emanating from the crack tip at an angle of 45° and taking into account that the limit load of a structure is directly related to the length of the slip-line in each material zone (Hao et al., 1997), the V-groove weld bevel geometry can be simplified to a square weld bevel whose width (h_{eq}) can be calculated from the intersection between the weld fusion line and the slip-line trajectory as illustrated in Fig. 2(b).

While the procedure outlined above is applicable to a bimaterial configuration, its extension to clad pipes is not performed in a straightforward manner as it is necessary to determine the influence of the clad layer thickness in the limit load of the structure. To this end, the clad pipe girth weld is modeled as a three material system illustrated in Fig. 2(c). Considering that a similar slip-line pattern develops from the crack tip for this configuration, the clad layer influence can be computed by creating an equivalent square groove weld whose width (h_{eq}^{clad}) is calculated from the

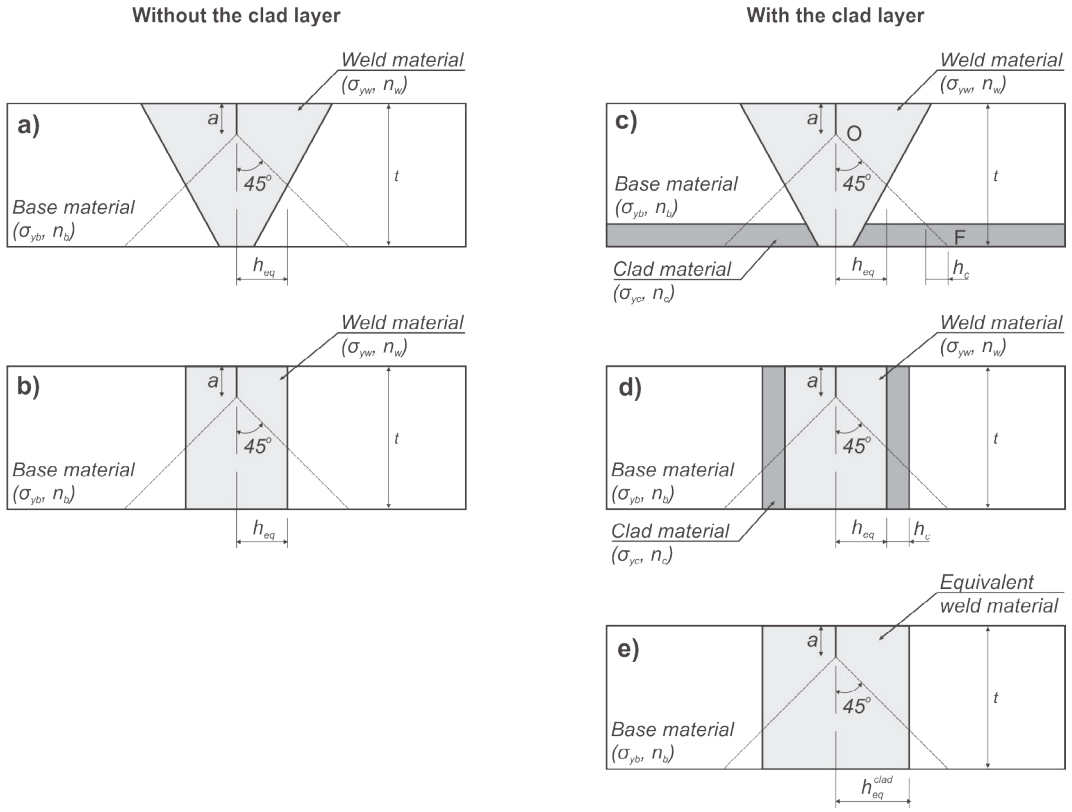

Fig. 2. Weld bevel simplification scheme for: (a,b) pipeline girth weld without a clad layer and (c-e) pipeline girth weld with a clad layer .

sum of the contributions of the weld and clad material zones $h_{eq}^{clad} = h_{eq} + h_c$ see Fig. 2(c) and (d). The equivalent weld material property is then computed from the following equation proposed by Hertelé et al. (2014):

$$M_{eq} = \frac{\int M(s)\, ds}{||OF||} \tag{3}$$

where M_{eq} denotes the equivalent mismatch ratio of the equivalent weld material including the clad layer, $M(s)$ is the mismatch ratio related to the length s and $||OF||$ is the total length of the straight line from point O to point F, as depicted in Fig. 2(c). Considering the occurrence of material mismatch in the entire stress-plastic strain range, Eq. (3) can be rewritten as

$$M_{eq}^{clad}(\varepsilon_p) = \frac{M_{wm}(\varepsilon_p) l_w + M_{cm}(\varepsilon_p) l_c}{l_w + l_c} \tag{4}$$

where l_w and l_c represent the length of the slip-line inside the weld and clad region and $M_{wm}(\varepsilon_p) = \sigma_{yw}(\varepsilon_p)/\sigma_{yb}(\varepsilon_p)$ and $M_{cm}(\varepsilon_p) = \sigma_{yc}(\varepsilon_p)/\sigma_{yb}(\varepsilon_p)$ are the mismatch ratio of the weld and clad material with respect to the base material. The above methodology described by Eq. (4) allows the representation of the complex clad pipe girth weld in a simplified two material configuration. It is worth mentioning that the assumption of a straight slip-line mechanism in both cases may not hold true as the deformation pattern may not follow a straight line depending on the weld size, structure geometry and mismatch level Hao et al. (1997). The validity of the method and its limitations will be addressed in section 5.1

4. Numerical Procedures and Material Models

The analysis matrix considers circumferentially cracked pipes with constant wall thickness $t = 20.6$ mm and outer diameters $D_e = 206$ mm and 412 mm ($D_e/t = 10$ and $D_e/t = 20$). Two clad layer thickness are employed in this study: $t_c = 1$ mm and 3 mm, which are representative of typical ranges in pipeline CRA layer thickness adopted in real engineering applications (Olso et al., 2011).

To investigate the weld bevel simplification procedure described in Section 3, two crack lengths ($\theta/\pi = 0.04$ and 0.2) and two crack depths ($a/t = 0.1$ and 0.5) are considered. The weld bevel includes a wide gap geometry with $\beta = 30°$, representative of typical manual welding procedures and a narrow gap with $\beta = 10°$, which represents welded joints fabricated with automatic processes (see Fig. 3(c-d)), with six levels of weld strength mismatch: $M_y = 0.5$, 0.8, 0.9, 1.1, 1.2 and 1.5. Both weld geometries have the same root width $h_r = 5$ mm.

The limit load analyses consider a material with yield stress $\sigma_{ys} = 500\,MPa$. Note that the value of the yield stress does not influence the limit load ratio P_0^{mism}/P_0^{bm}. The analyses also consider the following elastic properties: $E = 206\,GPa$ and $\upsilon = 0.3$. The limit load analyses employ a elastic-perfectly plastic stress *vs*. relationship described by

$$\frac{\bar{\epsilon}}{\epsilon_{ys}} = \frac{\bar{\sigma}}{\sigma_{ys}}\ ,\ \epsilon \leq \epsilon_{ys}\ ;\ \ \bar{\sigma} = \bar{\sigma}_{ys}\ ,\ \epsilon > \epsilon_{ys}. \tag{5}$$

The elastic-plastic analyses conducted for the validation study considers a typical pipe configuration with $D_e/t = 15$, $\theta/\pi = 0.12$, $a/t = 0.2$ and pipe wall thickness $t = 20$ mm. Wide and narrow gap weld geometries are employed in the analyses. The study also considers two clad layer thickness $t_c = 0$ and 2 mm. A typical pipeline steel (API 5L Grade X60) with $483\,MPa$ yield stress and strain hardening $n = 12$ is adopted (Chiodo and Ruggieri, 2010). To evaluate the effect of the weld and clad metal dissimilarity two mismatch levels are considered: $M_y = 1.15$ and $M_y = 0.85$ (here both weld and clad metal have the same strain hardening). The constitutive model follows a flow theory with conventional Mises plasticity in small geometry change (SGC) setting (Chiodo and Ruggieri, 2010). The elastic-plastic analyses utilize a simple power-hardening model to characterize the uniaxial true stress ($\bar{\sigma}$) *vs.* logarithmic strain ($\bar{\epsilon}$) in the form

$$\frac{\bar{\epsilon}}{\epsilon_{ys}} = \frac{\bar{\sigma}}{\sigma_{ys}}\ ,\ \epsilon \leq \epsilon_{ys}\ ;\ \ \frac{\bar{\epsilon}}{\epsilon_{ys}} = \left(\frac{\bar{\sigma}}{\sigma_{ys}}\right)^n\ ,\ \epsilon > \epsilon_{ys} \tag{6}$$

where σ_{ys} and ϵ_{ys} are the reference (yield) stress and strain, and n is the strain hardening exponent.

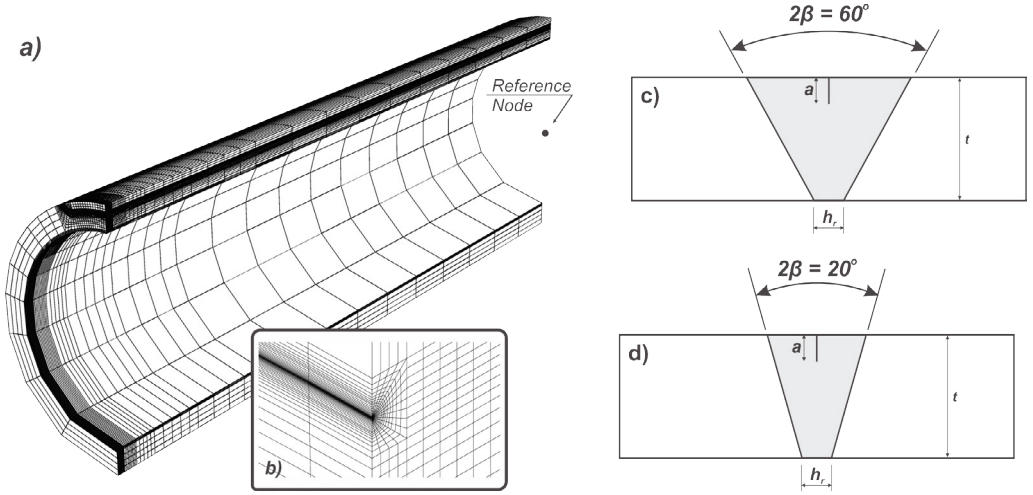

Fig. 3. Typical finite element model employed in the numerical analyses: (a) representation of the pipe mesh and the location of the reference node and (b) detail of the crack tip and the focused mesh configuration. Illustration of the weld bevel geometries adopted in this work: (a) wide gap weld with $\beta = 60°$ and (b) narrow gap weld with $\beta = 10°$.

Figure 3(a-b) shows a typical finite element model constructed for the pipe with $D_e/t = 10$, $\theta/\pi = 0.12$, $a/t = 0.3$. The models are built using a mesh generator created with Python programming language coupled with the finite element software Abaqus 6.12. The model is based on a plate which is subsequently mapped into the desired cylindrical geometry. The crack is modeled with a rectangular shape and constant depth through the entire crack length (Nourpanah and Taheri, 2010). A conventional mesh configuration having a focal mesh with ten concentric rings of elements surrounding the crack tip is used with the smallest element dimension being on the order of 10^{-2} mm. The crack tip is modeled with collapsed wedge elements which makes the crack ideally sharp initially, but allows it to blunt as deformation advances (Parise et al., 2015). To adequately capture the discontinuity effect of the crack, the pipe models were designed with a total length $L = 3D_e$. Due to symmetry, only one quarter of the pipe is modeled with appropriate constraints imposed on the nodes defining the symmetry planes.

Hexaedrical eight node isoparametrical elements with reduced integration and hourglass control (C3D8R) were employed in this work. CTOD is computed through the 90° intercept procedure at the maximum crack depth (Chiodo and Ruggieri, 2010). Pure bending moment is applied in the pipe configuration through a rotational displacement at a reference point located at the end of the pipe, as depicted in Fig. 3(a). The nodes at the end of the pipe are connected to the reference point using a multipoint constraint which distributes linearly the displacement originated from the applied rotation. The global strain, ε, applied in the pipe can be directly related to the imposed rotation in the form $\varphi = 2L\varepsilon/D_e$, where φ is the angle of rotation imposed in the reference point and L is the pipe length. The total bending moment in each step of the simulation is calculated from the sum of the contributions of each node located in the crack plane.

5. Results and discussion

5.1. Weld bevel simplification scheme

Figure 4 displays the ratio between the limit load of the pipe with an explicitly modeled V-groove weld $M_0^{mism}(V-groove)$ and the limit load of the pipe with an equivalent square groove weld $M_0^{mism}(Square-groove)$ for different levels of mismatch ratios and the following pipe geometries: $D_e/t = 10$, 20, $\theta/\pi = 0.04$, 0.20, $a/t = 0.1$, 0.5.

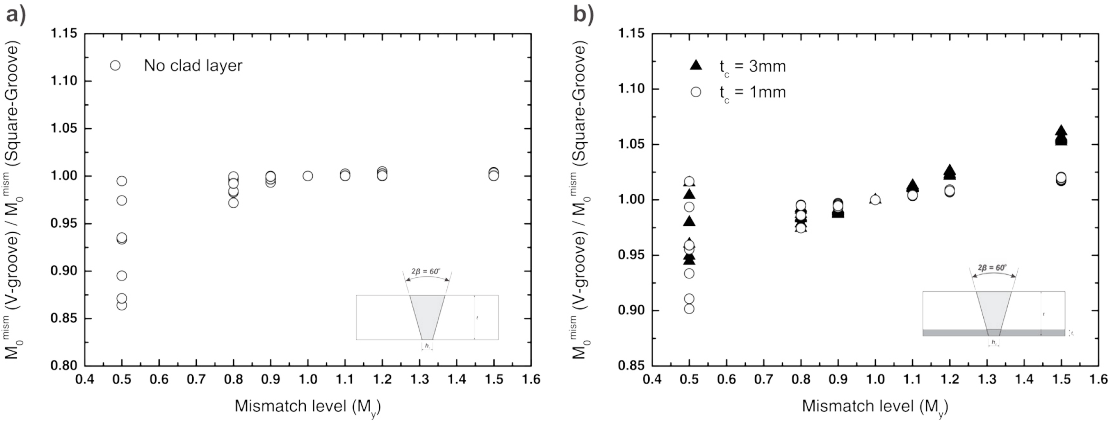

Fig. 4. Weld bevel simplification scheme for V-groove welds with $\beta = 30°$ and (a) no clad layer and (b) $t_c = 1$ mm and 3 mm.

Figure 4(a) shows the results for the weld bevel simplification scheme applied to wide V-groove weld ($\beta = 30°$) and no clad layer. It can be seen that the simplification procedure is adequate for all geometries and the following mismatch levels: $M_y = 0.8$, 0.9, 1.1, 1.2 and 1.5. Within this range, the difference between the limit loads for a a pipe with a V-groove weld and the respective simplified square weld is less than ±5 %. While the simplification procedure results in a good approximation for those mismatch levels, the method is not applicable in the presence of high levels of weld strength undermatch $M_y = 0.5$. In this case, the deformation pattern changes significantly, resulting in a poor agreement between the limit load of the actual weld and the idealised square geometry. The same trend is observed for the cladded pipes as illustrated in Fig. 4(b).

The results of the weld bevel simplification procedure considering the narrow gap V-weld geometry ($\beta = 30°$) are similar to the wide gap weld and not shown here in interest of space. Again, a more pronounced difference also occurs in the case of extreme undermatch.

5.2. Evolution of CTOD with applied bending moment

This section presents a validation study considering the analyses matrix depicted in Section 4. The following procedure is adopted in the case study:

- the V-groove weld is simplified to a square groove geometry, according to the procedure outlined in Section 3;
- the equivalent stress *vs*. strain curve is determined using Eq. (1) and the limit load solutions for pipes with finite circumferential part-through internal crack at the girth weld subjected to tension load (Kim et al., 2009), as detailed in Section 3;
- the Ramberg-Osgood parameters of the equivalent curve (n and σ_{ys}) are determined through interpolation;
- the evolution of CTOD with applied bending moment is determined through the application of the EPRI approach using the h_2-values described in details by Souza et al. (2016).

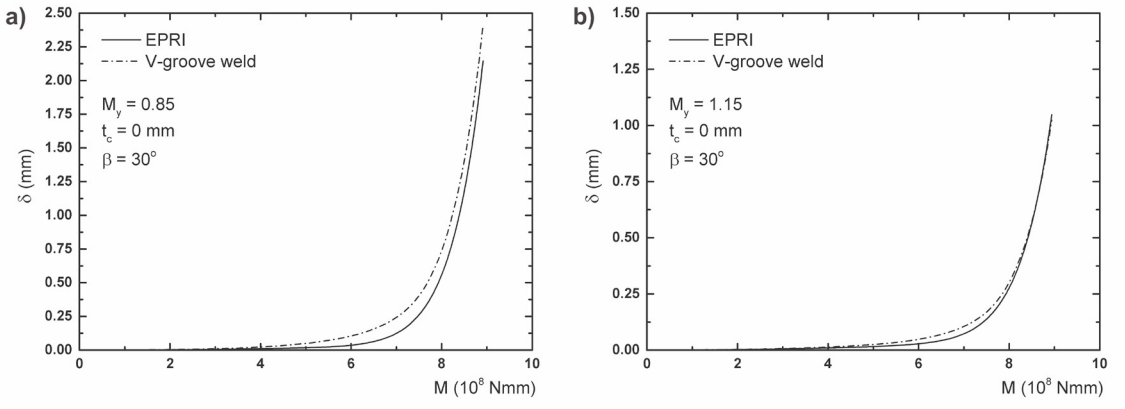

Fig. 5. Comparison of the CTOD values obtained through the EPRI/ESSRM framework and finite element results for a pipe with $D_e/t = 15$, $\theta/\pi = 0.12$, $a/t = 0.2$, $\beta = 30°$, $t_c = 0$ mm for (a) $M_y = 0.85$ and (b)$M_y = 1.15$.

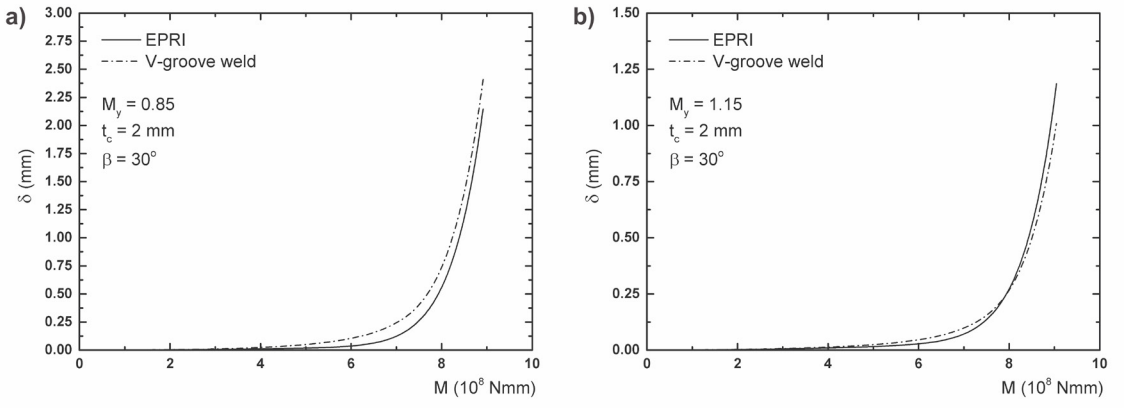

Fig. 6. Comparison of the CTOD values obtained through the EPRI/ESSRM framework and finite element results for a pipe with $D_e/t = 15$, $\theta/\pi = 0.12$, $a/t = 0.2$, $\beta = 30°$, $t_c = 2$ mm for (a) $M_y = 0.85$ and (b)$M_y = 1.15$.

Figures 5 and 6 show CTOD estimations for the pipe with a wide gap girth weld, t_c = 0 and 2 mm and M_y = 1.15 and M_y = 0.85. Despite small deviations between the CTOD predictions at low levels of plasticity, there is very good agreement between the crack driving forces evolution for both mismatch levels in fully plastic conditions ($CTOD >$ 0.5 mm). The results are similar to the narrow gap condition. The CTOD estimation is very accurate in the fully plastic condition for all the cases.

6. Concluding Remarks

This work presents a framework for structural integrity assessment of dissimilar girth welds in offshore clad pipes under bending, based on the equivalent stress-strain relationship approach coupled with the EPRI methodology and a weld groove simplification procedure. The 3-D finite element analyses of circumferentially surface cracked pipes performed in this work validates the V-groove joint simplification into a square geometry for mismatch levels M_y = 0.8 to 1.5. Application of the ESSRM coupled with the weld geometry simplification allows the representation of a complex trimaterial system into a homogeneous structure composed by only one equivalent material which permits the application of standard fracture integrity assessment methods. Finally, verification studies are performed using the EPRI crack driving force estimation procedure based on h_2-values specifically developed to the crack geometry employed in this work. Parametric analyses demonstrate that the evolution of CTOD with bending moment is very well predicted by the new method when compared to finite element simulations of the actual main features.

Acknowledgments

This investigation was supported by the Brazilian Council for Scientific and Technological Development (CNPq) through Grant 200506/2014-5. The first author acknowledge Prof. Zhiliang Zhang from NTNU for providing support for the work described here. The authors are also indebted to Dr. Eduardo Hippert Jr. (Petrobras) for providing the motivation to this work and for the many helpful discussions on ECA procedures.

References

American Petroleum Institute, 2007. Fitness-for-service, API RP-579-1 / ASME FFS-1.

Anderson, T.L., 2005. Fracture Mechanics: Fundaments and Applications - 3rd Edition. CRC Press, Boca Raton, FL.

British Institution, 2013. Guide to methods for assessing the acceptability of flaws in metallic structures, BS 7910.

Chiesa, M., Nyhus, B., Skallerud, B., Thaulow, C., 2001. Efficient fracture assessment of pipelines: A constraint-corrected sent specimen approach. Engineering Fracture Mechanics 68, 527–547.

Chiodo, M.S.G., Ruggieri, C., 2010. J and CTOD estimation procedure for circumferential surface cracks in pipes under bending. Engineering Fracture Mechanics 77, 415–436.

Hao, S., Cornec, A., Schwalbe, K.H., 1997. Plastic stress-strain fileds and limit loads of a plane strain cracked tensile panel with a mismatched welded joint. International Journal of Solids and Structures 34, 297–326.

Hertelé, S., Waele, W.D., Verstrate, M., Denys, R., O'Dowd, N., 2014. J -integral analysis of heterogeneous mismatched girth welds in clamped single-edge notched tension specimens. International Journal of Pressure Vessel and Piping 119, 95–107.

Kim, J.S., Song, T.K., Kim, Y.J., Jin, T.E., 2009. Strength mismatch effect on limit load for circumferential surface cracked pipes. Engineering Fracture Mecjanics , 12.

Kumar, V., German, M.D., Shih, C.F., 1981. An Engineering Approach to Elastic-Plastic Fracture Analysis. Technical Report EPRI NP-1931. Electric Power Research Institute. Palo Alto, CA.

Lei, Y., Ainsworth, R.A., 1997. The estimation of J in three-point-bend specimens with a crack in a mismatched weld. International Journal of Pressure Vessel and Piping 70, 247–257.

Manouchehri, S., 2012. A discussion of practical aspects of reeled flowline installation, in: 31st International Conference on Ocean, Offshore and Arctic Engineering (OMAE 2012) , American Society of Mechanical Engineers, Rio de Janeiro, Brazil.

Nourpanah, N., Taheri, F., 2010. Development of a reference strain approach for assessment of fracture response of reeled pipelines. Eng. Fract. Mech. 77, 2337–2353.

Olso, E., Berg, E., Nyhus, B., Thaulow, C., Ostby, E., 2011. A new assessment approach for ECA of clad and lined pipes based on shell and line-spring finite elements, in: Proceedings of the Twenty-first (2011) International Offshore and Polar Engineering Conference.

Parise, L.F.S., Ruggieri, C., O'Dowd, N., 2015. Fully plastic strain-based J estimation scheme for circumferential surface cracks in pipes subjected to reeling. Journal of Pressure Vessel Technology 137, 100–108.

Souza, R.F., Ruggieri, C., Zhang, Z., 2016. A framework for fracture assessment of dissimilar girth welds in offshore pipelines under bending. Engineering Fracture Mechanics , Submitted for Publication.